Novel Gallium Phosphatooxalate with Pendant Oxalate Ligands: Preparation, Crystal Structure, NMR Spectroscopy, and Thermal Stability

Charlotte T. S. Choi,[†] Ekaterina V. Anokhina,[†] Cynthia S. Day,[†] Yue Zhao,[†] Francis Taulelle,[‡] Clarisse Huguenard,[‡] Zhehong Gan,[§] and Abdessadek Lachgar*[,†]

Department of Chemistry, Wake Forest University, Winston-Salem, North Carolina 27109-7486, RMN et Chimie du Solide, Université Louis Pasteur, 4, rue Blaise Pascal, 67070 Strasbourg, France, and Center of Interdisciplinary Magnetic Resonance, National High Magnetic Field Laboratory, 1800 East Paul Dirac Drive, Tallahassee, Florida 32310

Received April 16, 2002. Revised Manuscript Received July 22, 2002

A new gallium phosphatooxalate hybrid material, $(C_{10}H_{28}N_4)[Ga_6(OH)_2(PO_4)_2(HPO_4)_4(C_2O_4)_3]\cdot 3.5H_2O$ (**1**), has been synthesized under mild hydrothermal conditions (150 °C) in the presence of the amine 1,4-bis(3-aminopropyl)piperazine (APPIP) as a structure-directing agent. The compound was structurally characterized by single-crystal X-ray diffraction, thermogravimetric analysis, and ^1H, ^2H, ^{13}C, ^{31}P, and ^{71}Ga solid-state NMR spectroscopy. The structure of (**1**) consists of gallium phosphate double layers formed of GaO_6 octahedra, GaO_4 tetrahedra, and HPO_4 and PO_4 groups sharing corners. The double layers are cross-linked by oxalate ligands to form a three-dimensional framework with intersecting channels where the amine and water molecules are located. The oxalate units play a dual role as nonbridging mono-bidentate ligands with two terminal C−O groups pendant inside the channels and bis-bidentate ligands bridging the double layers. Crystal data are as follows: triclinic $P\bar{1}$ (No. 2), $a = 9.0220(7)$ Å, $b = 9.1864(9)$ Å, $c = 13.4912(9)$ Å, $\alpha = 73.988(9)°$, $\beta = 79.199(7)°$, $\gamma = 78.775(7)°$, $V = 1043.6(2)$ Å^3, and $Z = 1$. ^{71}Ga MAS NMR confirms the presence of four- and six-coordinated Ga atoms. Three ^{31}P resonances at −0.2, −4.15, and −7.7 ppm in a 1:1:1 ratio are observed, consistent with the structural model determined from the XRD structural analysis. Thermogravimetric analysis and X-ray diffraction show that the framework is stable up to about 300 °C after complete dehydration. The compound partially reabsorbs water, giving a cell volume intermediate between the completely hydrated and dehydrated phase.

Introduction

The discovery of aluminophosphates (AlPOs) with zeolite-like structures and their potential applications in catalysis, ion exchange, and gas separation led to extensive research activity in the field of open-framework metal phosphates.[1−4] Investigation of gallium phosphates led to the discovery of many new structural types not found in AlPOs.[5−16] These materials are generally prepared in the presence of an organic ammonium cation, which is occluded within the anionic inorganic framework and plays the role of a structure-directing agent (SDA).[1,17,18]

In recent years, parallel to the expansion in the research of oxide-based open-framework materials, significant progress has been made in the area of porous coordination solids whose structures are formed from molecular building blocks held together through suitable multidentate organic ligands.[19−25] The recent approach of combining the robustness of inorganic frameworks

* To whom correspondence should be addressed.
[†] Wake Forest University.
[‡] Université Louis Pasteur.
[§] National High Magnetic Field Laboratory.

(1) Wilson, S. T.; Lok, B. M.; Messina, C. A.; Cannan, T. R.; Flanigen, E. M. *J. Am. Chem. Soc.* **1982**, *104*, 1146−1147.
(2) Wilson, S. T.; Woodward, N. A.; Flanigen, E. M.; Eggert, H. G. Union Carbide, EU-B 226219, 1987.
(3) Kniep, R. *Angew. Chem., Int. Ed. Engl.* **1986**, *25*, 525−534.
(4) Cheetham, A. K.; Férey, G.; Loiseau, L. *Angew. Chem., Int. Ed.* **1999**, *38*, 3268−3292.
(5) Parise, J. B. *J. Chem. Soc., Chem. Commun.* **1985**, *9*, 606−607.
(6) Yang, G.; Feng, S.; Xu, R. *J. Chem. Soc., Chem. Commun.* **1987**, *16*, 1254−1255.
(7) Estermann, E.; McCusker, L. B.; Baerlocher, C.; Merrouche, A.; Kessler, H. *Nature* **1991**, *352*, 320−323.
(8) Jones, R. H.; Thomas, J. M.; Huo, Q.; Xu, R.; Hursthouse, M. B. *J. Chem. Soc., Chem. Commun.* **1991**, *21*, 1520−1522.
(9) Attfield, M. P.; Morris, R. E.; Gutierrez-Puebla, E.; Monge-Bravo, A.; Cheetham, A. K. *J. Chem. Soc., Chem. Commun.* **1995**, *8*, 843−844.
(10) Feng, S.; Xu, X.; Yang, G.; Xu, R.; Glasser, F. P. *J. Chem. Soc., Dalton Trans.* **1995**, *13*, 2147−2149.
(11) Chippindale, A. M.; Walton, R. I.; Turner, C. *J. Chem. Soc., Chem. Commun.* **1995**, *12*, 1261−1262.
(12) Lii, K.-H. *Inorg. Chem.* **1996**, *35* (25), 7440−7442.
(13) Loiseau, T.; Serpaggi, F.; Férey G. *J. Chem. Soc., Chem. Commun.* **1997**, *12*, 1093−1094.
(14) Lin, H.-M.; Lii, K.-H. *Inorg. Chem.* **1998**, *37* (17), 4220−4222.
(15) Hsu, K.-F.; Wang, S.-L. *Inorg. Chem.* **2000**, *39* (8), 1773−1778.
(16) Lin, C.-H.; Wang, S.-L.; Lii, K.-H. *J. Am. Chem. Soc.* **2001**, *123* (19), 4649−4650.
(17) Haushalter, R. C.; Mundi, L. A. *Chem. Mater.* **1992**, *4* (1), 31−48.
(18) Férey, G. *C. R. Acad. Sci. Ser. C* **1998**, *1*, 1−13.

10.1021/cm020389k CCC: $22.00
Published on Web 10/02/2002

with the versatility and chemical flexibility of organic ligands has led to a number of novel hybrid inorganic−organic open-framework materials, such as phosphonates, phosphono-aminocarboxylates, and phosphatodicarboxilates.[26−28] In the latter category, the use of oxalate, C_2O_4, as a bridging bidentate ligand has been investigated by a number of research groups and led to the preparation of hybrid phosphatooxalates of V,[29−32] Mn,[30,33,34] Fe,[35−42] Co,[43] Zn,[44] Mo,[45] Al,[46,47] Ga,[48−50] In,[51] and Sn.[52,53] In most cases, the frameworks of these materials are built of metal phosphate layers bridged by oxalate ligands. The incorporation of oxalate units within the inorganic layer has been observed in a few cases only.[42,43,48−51,54]

In the gallium system, Lii and co-workers reported three gallium phosphatooxalates with interesting structural properties: $[Ga_5(OH)_2(C_{10}H_9N_2)(C_2O_4)(PO_4)_4]\cdot 2H_2O$,[48] which consists of GaO_4 tetrahedra and GaO_6 octahedra linked by phosphate and oxalate groups to form hybrid inorganic−organic layers that are bridged by GaO_4N trigonal bipyramids to produce a three-dimensional (3D) framework; $(R\text{-}C_5H_{14}N_2)_2[Ga_4(C_2O_4)(H_2PO_4)_2(PO_4)_4]\cdot 2H_2O$,[49] the first phosphatooxalate templated with a chiral amine, which consists of GaO_6 octahedra and GaO_4 tetrahedra linked by C_2O_4 and PO_4 groups to form hybrid inorganic−organic layers that interact through the protonated amine; and $K_2[Ga_4(C_2O_4)(PO_4)_4]\cdot 2H_2O$,[50] which is built of GaO_6 octahedra and GaO_4 tetrahedra connected by coordinating C_2O_4 and PO_4 units to generate a three-dimensional framework with intersecting channels where water molecules and potassium cations are located. We have prepared a new open-framework gallium phosphatooxalate, $(C_{10}H_{28}N_4)[Ga_6(OH)_2(PO_4)_2(HPO_4)_4(C_2O_4)_3]\cdot 3.5H_2O$ (**1**), that has a 3D structure built of gallium phosphate double layers connected by oxalate units. Two types of oxalate units are present; one type acts as bridging ligands and chelates two gallium centers while the other C_2O_4 unit chelates only one gallium atom and has two terminal C−O groups pendant inside 12-ring channels. In this paper, its synthesis, crystal structure, solid-state NMR, and TG analysis are presented.

Experimental Section

General Procedures. All reactions were performed under hydrothermal conditions, with the following: Ga_2O_3 (99.99%, Alfa), 1,4-bis(3-aminopropyl)piperazine ($C_{10}N_4H_{24}$) (APPIP) (97%, Aldrich), ($H_2C_2O_4.2H_2O$) (99%, Aldrich), H_3PO_4 (85%, Fisher), and reagent-grade HCl and H_2SO_4 (Fisher).

Synthesis and Preliminary Characterization. 1 was prepared starting from a mixture containing Ga_2O_3, $H_2C_2O_4.2H_2O$, H_3PO_4, APPIP, HCl (3 M), and H_2O at a molar ratio of 1:1:4:2:6:400. In a typical synthesis, 0.158 g of Ga_2O_3 was dispersed in 4.3 mL of water and 1.7 mL of HCl (3 M) under stirring; 0.23 mL of H_3PO_4 (aqueous 85 wt %), 0.106 g of $H_2C_2O_4.2H_2O$, and 0.36 mL of APPIP were added with continuous stirring and the mixture was homogenized for ≈30 min. The starting mixture (≈7 mL) was transferred to a 23-mL capacity PTFE-lined stainless steel autoclave (Parr, Moline, IL) sealed and heated at 150 °C for 68 h under autogenous pressure followed by slow cooling to room temperature at 10 °C/h. The pH of the mixture remained practically unchanged (≈1.3). The resulting product consisted of colorless plate-shaped crystals of (**1**) obtained in 88.2% yield based on Ga was filtered and washed with deionized water and acetone and dried in air. Deuteurated samples for solid-state NMR were prepared using concentrated H_2SO_4 and D_2O. The calculated percentage of deuteuration was ≈94.6%. Elemental analysis confirmed the number of tetraprotonated APPIP, oxalates, and water molecules per formula unit. Found: C, 12.46; N, 3.53; H, 2.61. Calcd: C, 12.34; N, 3.60; H, 2.65.

Crystal Structure Analysis. The crystal structure of (**1**) was determined by single-crystal X-ray diffraction methods. Preliminary studies and data collection were performed at 228(2) K on a platelike single crystal of (**1**) using a Bruker P4 diffractometer. Crystallographic details are listed in Table 1. Initial positional parameters for gallium, phosphorus, and oxygen atoms were determined using direct methods, and the

(19) Eddaoudi, M.; Moler, D. B.; Li, H. L.; Chen, B. L.; Reineke, T. M.; O'Keeffe, M.; Yaghi, O. M. *Acc. Chem. Res.* **2001**, *34*, 319−330.
(20) Yaghi, O. M.; Li, H. L.; Davis, C.; Richardson, D.; Groy, T. L. *Acc. Chem. Res.* **1998**, *31*, 474−484.
(21) Abrahams, B. F.; Hoskins, B. F.; Michail, D. M.; Robson, R. *Nature* **1994**, *369*, 727−729.
(22) MacGillivray, L. R.; Subramanian, S.; Zaworotko, M. J. *J. Chem. Soc., Chem. Commun.* **1994**, *11*, 1325−1326.
(23) Gardner, G. B.; Venkataraman, D.; Moore, J. S.; Lee, S. *Nature* **1995**, *374*, 792−795.
(24) Gutschke, S. O. H.; Molinier, M.; Powell, A. K.; Winpenny, R. E. P.; Wood, P. T. *J. Chem. Soc., Chem. Commun.* **1996**, *7*, 823−824.
(25) Hagrman, P. J.; Hagrman, D.; Zubieta, J. *Angew. Chem., Int. Ed.* **1999**, *38*, 2638−2684.
(26) Drumel, S.; Janvier, P.; Barboux, P.; Bujoli-Doeuff, M.; Bujoli, B. *Inorg. Chem.* **1995**, *34*, 148. Hix, G. B.; Wragg, D. S.; Wright, P. A.; Morris, R. E. *J. Chem. Soc., Dalton Trans.* **1998**, 3359−3361.
(27) Hartman, S. J.; Todorov, E.; Cruz, C.; Sevov, S. C. *Chem. Commun.* **2000**, 1213−1214.
(28) Distler, A.; Sevov, S. C. *Chem. Commun.* **1998**, *9*, 959. Serpaggi, F.; Férey, G. *Inorg. Chem.* **1999**, *38*, 4741. Ayyappan, S.; de Delgado, G. D.; Cheetham, A. K.; Férey, G.; Rao, C. N. R. *J. Chem. Soc., Dalton Trans.* **1999**, 2905.
(29) Tsai, Y.-M.; Wang, S.-L.; Huang, C.-H.; Lii, K.-H. *Inorg. Chem.* **1999**, *38* (19), 4183−4187.
(30) Law, T. S-C.; Sung, H. H-Y.; Williams, I. D. *Inorg. Chem. Commun.* **2000**, *3*, 420−423.
(31) Do, J.; Bontchev, R. P.; Jacobson, A. J. *Inorg. Chem.* **2000**, *39*, 3230−3237.
(32) Do, J.; Bontchev, R. P.; Jacobson, A. J. J. *Chem. Mater.* **2001**, *13*, 2601−2607.
(33) Lethbridge, Z. A. D.; Tiwary, S. K.; Harrison, A.; Lightfoot, P. *J. Chem. Soc., Dalton Trans.* **2001**, *12*, 1904−1910.
(34) Lethbridge, Z. A. D.; Hillier, A. D.; Cywinski, R.; Lightfoot, P. *J. Chem. Soc., Dalton Trans.* **2000**, 1595−1599.
(35) Natarajan, S. *Proc. Indian Acad. Sci.* (*Chem. Sci.*) **2000**, *112* (3), 249−272.
(36) Lin, H.-M.; Lii, K.-H.; Jiang, Y.-C.; Wang, S.-L. *Chem. Mater.* **1999**, *11* (3), 519−521.
(37) Chang, W.-J.; Lin, H.-M.; Lii, K.-H. *J. Solid State Chem.* **2001**, *157* (1), 233−239.
(38) Lethbridge, Z. A. D.; Lightfoot, P. *J. Solid State Chem.* **1999**, *143* (1), 58−61.
(39) Choudhury, A.; Natarajan, S.; Rao, C. N. R. *J. Solid State Chem.* **1999**, *146* (2), 538−545.
(40) Choudhury, A.; Natarajan, S.; Rao, C. N. R. *Chem. Mater.* **1999**, *11*, 2316−2318.
(41) Choudhury, A.; Natarajan, S. *J. Mater. Chem.* **1999**, *9* (12), 3113−3117.
(42) Choudhury, A.; Natarajan, S.; Rao, C. N. R. *Chem. Eur. J.* **2000**, *6* (7), 1168−1175.
(43) Choudhury, A.; Natarajan, S. *Solid State Sci.* **2000**, *2*, 365−372.
(44) Neeraj, S.; Natarajan, S.; Rao, C. N. R. *J. Chem. Soc., Dalton Trans.* **2001**, 289−291.
(45) Lee, M.-Y.; Wang, S.-L. *Chem. Mater.* **1999**, *11*, 3588−3594.
(46) Lightfoot, P.; Lethbridge, Z. A. D.; Morris, R. E.; Wragg, D. S.; Wright, P. A.; Kvick, A.; Vaughan, G. B. M. *J. Solid State Chem.* **1999**, *143* (1), 74−76.
(47) Kedarnath, K.; Choudhury, A.; Natarajan, S. *J. Solid State Chem.* **2000**, *150* (1), 324−329.
(48) Chen, C.-Y.; Chu, P. P.; Lii, K.-H. *J. Chem. Soc., Chem. Commun.* **1999**, 1473−1474.
(49) Lii, K.-H.; Chen, C.-Y. *Inorg. Chem.* **2000**, *39* (15), 3374−3378.
(50) Hung, L.-C.; Kao, H.-M.; Lii, K.-H. *Chem. Mater.* **2000**, *12* (8), 2411−2417.
(51) Huang, Y.-F.; Lii, K.-H. *J. Chem. Soc., Dalton Trans.* **1998**, 4085−4086.
(52) Natarajan, S. *J. Solid State Chem.* **1998**, *139* (1), 200−203.
(53) Adair, B.; Natarajan, S.; Cheetham, A. K. *J. Mater. Chem.* **1998**, *8*, 1477.
(54) Choi, C.; Anokhina, E. V.; Piffard, Y.; Lachgar, A. *Chem. Mater.*, in preparation.

Table 1. Crystal and Structure Refinement Data for $[N_4C_{10}H_{28}]$ $[Ga_6(OH)_2(PO_4)_2(HPO_4)_4(C_2O_4)_3]\cdot 3.5H_2O$

fw (g/mol)	778.83	V (Å^3)	1043.5(2)
crystal system	triclinic	Z	1
space group	$P\bar{1}$ (No. 2)	ρ_{calcd} (g cm^{-3})	2.479
a (Å)	9.0220(7)	μ (mm^{-1})	4.19
b (Å)	9.1864(9)	λ (Å)	0.71073
c (Å)	13.4912(9)	T (K)	228(2)
α (deg)	73.988(9)	R1[a]	0.045
β (deg)	79.199(7)	wR2[b,c]	0.066
γ (deg)	78.775(7)	GOF	1.026

[a] $R1 = \Sigma||F_o| - |F_c||/\Sigma|F_o|$ (for all data). [b] $wR_2 = [\Sigma[w(F_o^2 - F_c^2)^2]/\Sigma[(wF_o^2)^2]]^{1/2}$ for all data. [c] $w^{-1} = \sigma^2(F_o^2) + (0.0287P)^2 + 1.3168P$ where $P = (\mathrm{Max}(F_o^2, 0) + 2F_c^2)/3$.

structure was refined using full-matrix least-squares techniques (Bruker AXS SHELXTL).[55] A model containing all nonhydrogen atoms with anisotropic thermal parameters was refined to R1 = 0.048 and wR2 = 0.079 for all 6075 reflections. The three independent water oxygen atoms were included in the refinement with occupancy factors of 1.00, 0.50, and 0.25 for O(1w), O(2w), and O(3w), respectively. The hydrogen atoms (except those on the methyl groups) were located by a Fourier synthesis and refined isotropically. The resulting structural parameters were refined to R1 = 0.045 and wR2 = 0.066. Table 2 lists the most important bond distances and angles. Refinement in the space group $P1$ did not lead to new features. Positional parameters and equivalent isotropic thermal parameters and additional crystallographic results are given in the Supporting Information.

Thermal Analysis. Thermogravimetric analysis was carried out between 25 and 1000 °C under a flow of air or pure nitrogen with a heating rate of 10 °C min^{-1} using a Perkin-Elmer Pyris thermal analyzer.

Solid-State NMR Measurements. NMR spectra were acquired on a Bruker DSX 500 spectrometer with a 11.7-T field for ^{1}H, ^{2}H, ^{13}C, and ^{31}P nuclei. ^{71}Ga NMR was acquired on a 833-MHz field at NHMFL with a specific Bruker attached console. MAS probes used were Bruker 4 mm, 2.5 mm, and a Tallinn Probe of 2 mm for ^{71}Ga. The internal references used were as follows: for P, H_3PO_4/H_2O 85%; for H and C, TMS; for Ga, $Ga(NO_3)_3$ in water. The secondary external references used were as follows: for P, $(NH_4)H_2PO_4$; for H and C, adamantane; for Ga, Ga_2O_3. Specific conditions of acquisition and pulse sequences used are given in Supporting Information.

Results and Discussion

Structure Description. The structure of (**1**) (Figure 1) consists of gallium phosphate double layers parallel to the (*ab*) plane, cross-linked by oxalate ligands to form an anionic three-dimensional framework with intersecting tunnels parallel to the [100] and [010] directions where the cations $(H_4APPIP)^{4+}$ and water molecules are located (Figures 2 and 3). The gallium phosphate double layers are formed of two identical sublayers related to each other by inversion center. The sublayers contain two crystallographically independent GaO_6 octahedra, one GaO_4 tetrahedron, two HPO_4 tetrahedra, and one PO_4 tetrahedron. The two octahedrally coordinated gallium atoms Ga(1) and Ga(3) are linked via a μ-hydroxo ligand O(7)H, P(1)O_4, and HP(2)O_4 to form $Ga_2O_6(OH)(PO_4)(HPO_4)$ units. These dimeric units link to each other through HP(3)O_4 tetrahedra to form linear chains running along the [100] direction (Figure 4). The chains are, in turn, connected in the [010] direction via Ga(2)O_4 tetrahedra to generate the layers. The Ga(2)O_4 tetrahedron shares its two remaining oxygens to connect two symmetry-related sublayers and generate the double layers shown in Figure 4. The double layers are connected by oxalate anions that act as bis-bidentate ligands to two Ga(3) from two adjacent double layers.

The environment of the two octahedral gallium atoms Ga(1) and Ga(3) are chemically similar, each being coordinated by two oxygens from a bidentate oxalate ligand, one oxygen from the μ-hydroxo ligand O(7), and three oxygen atoms from three coordinating phosphate tetrahedra (two HPO_4 and one PO_4). There are two types of oxalate anions: one oxalate coordinates Ga(1) and acts as a mono-bidentate ligand through O(1) and O(2) with Ga(1)−O(1) = 1.974(2) Å and Ga(1)−O(2) = 1.992(2) Å and $(C-O)_{ave.}$ = 1.283(3) Å. The two terminal oxygens O(3) and O(4) have significantly shorter carbon−oxygen bond lengths with $(C-O)_{ave.}$ = 1.235(3) Å. The oxygen O(4) is involved in hydrogen bonding with the μ-hydroxo ligand O(4)- - -O(7) = 2.726(3) Å and O(4)- - -H(7) = 1.99 Å (Table 3). The other oxalate unit acts a bridge between adjacent double layers by chelating two Ga(3) from two different layers. The bis-bidentate coordination by the oxalate ligand results in a distorted octahedron for Ga(3), as indicated by a wide range of Ga(3)−O bond lengths 1.920(2)−2.049(2) Å and a small bond angle O(5)−Ga(3)−O(6) = 81.43(8)°. Three different coordinating phosphate groups are present: P(1)O_4 shares all its oxygens with gallium atoms: two with the tetrahedral Ga(2) atom and one with each octahedral gallium (Ga(1) and Ga(3)) in the same dimer; HP(2)O_4 shares one oxygen with each octahedrally coordinated gallium atom (O(21) with Ga(1) and O(22) with Ga(3)) and one oxygen with Ga(2). The fourth oxygen O(23) corresponds to an OH group with long P(2)−O(23) = 1.580(2) Å; the phosphate group HP(3)O_4 links two dimers within the same chain by sharing its oxygens O(32), O(33), and O(34) with Ga(1), Ga(3), and Ga(2), respectively.

The structure-directing cations $(H_4APPIP)^{4+}$ and water molecules O(1w) and O(3w) are located at the intersections of 12-membered ring (||[100]) and 10-membered ring (||[010]) channels running between the double layers. The channels in the [100] direction have windows formed by four GaO_6 octahedra, two GaO_4 tetrahedra, four HPO_4 tetrahedra, and two bridging oxalates, while the windows of the channels in the [010] direction are formed by six GaO_6 octahedra, two HPO_4 tetrahedra, and two bridging oxalates. A third type of channel formed by two GaO_6, two GaO_4, two PO_4, and two HPO_4 polyhedra is located within the double layers parallel to the [010] direction and contains the water molecule O(2w). The amine and water molecules form an extensive hydrogen-bonding network (Table 3). APPIP is hydrogen-bonded with all three phosphate groups and the nonbridging oxalate ligand, while O(1w) forms hydrogen bonding to O(3w), and to O(23). The water molecule O(2w) is involved in hydrogen bonding with one phosphate group only through O(13).

Thermogravimetric Analysis. Compound (**1**) showed similar weight loss under O_2 and under N_2 in the temperature range 20−1000 °C. Two distinct mass losses have been observed. The first mass loss (3.97%) occurs between 100 and 275 °C and corresponds to the loss of 3.5 H_2O (calcd 4.05%). X-ray diffraction studies

(55) Sheldrick, G. M. *SHELXTL Programs*, Version 5.1; Bruker AXS, 1998.

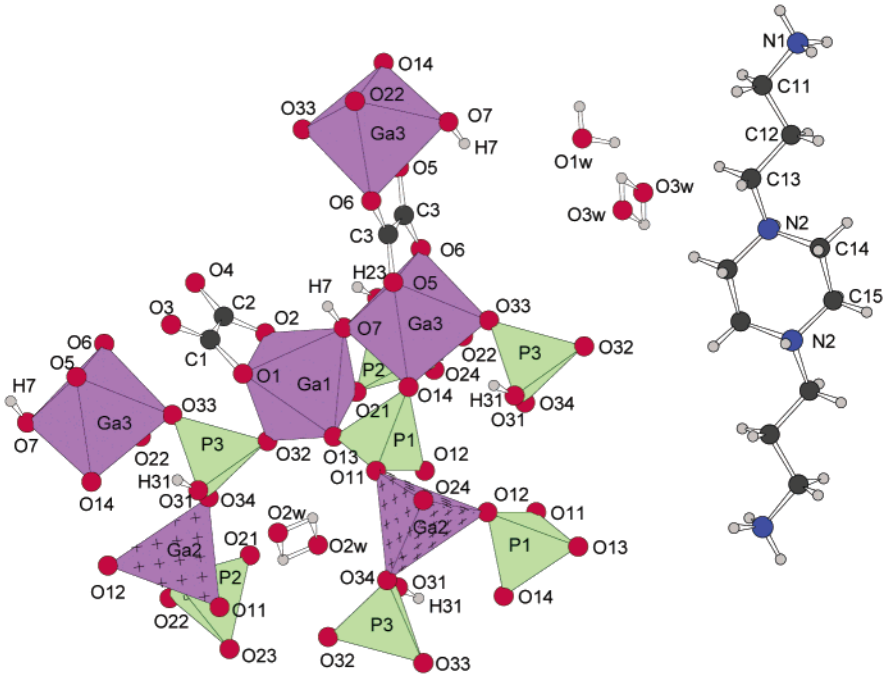

Figure 1. Fragment of the structure of **1** showing the atom labeling scheme and connectivities.

Table 2. Selected Interatomic Distances (Å) and Angles (deg) for $[N_4C_{10}H_{28}]$ $[Ga_6(OH)_2(PO_4)_2(HPO_4)_4(C_2O_4)_3]\cdot 3.5H_2O$

$Ga(1)O_6$ Octahedron		$Ga(2)O_4$ Tetrahedron		$Ga(3)O_6$ Octahedron	
Ga(1)−O(1)	1.974(2)	Ga(2)−O(11)	1.814(2)	Ga(3)−O(5)	2.033(2)
Ga(1)−O(2)	1.992(2)	Ga(2)−O(12)	1.810(3)	Ga(3)−O(6)	2.049(2)
Ga(1)−O(7)	1.957(2)	Ga(2)−O(24)	1.816(2)	Ga(3)−O(7)	1.939(2)
Ga(1)−O(13)	1.948(2)	Ga(2)−O(34)	1.807(2)	Ga(3)−O(14)	1.920(2)
Ga(1)−O(21)	1.969(2)			Ga(3)−O(22)	1.952(2)
Ga(1)−O(32)	1.961(2)			Ga(3)−O(33)	1.951(2)
$P(1)O_4$ Tetrahedron		$HP(2)O_4$ Tetrahedron		$HP(3)O_4$ Tetrahedron	
P(1)−O(11)	1.547(2)	P(2)−O(21)	1.516(2)	P(3)−O(31)	1.563(2)
P(1)−O(12)	1.550(2)	P(2)−O(22)	1.518(2)	P(3)−O(32)	1.508(2)
P(1)−O(13)	1.518(2)	P(2)−O(23)	1.580(2)	P(3)−O(33)	1.520(2)
P(1)−O(14)	1.514(2)	P(2)−O(24)	1.523(2)	P(3)−O(34)	1.554(2)

Ga−O−P Interpolyhedra Bond Angles (deg)			
Ga(1)−O(13)−P(1)	133.02(12)	Ga(2)−O(24)−P(2)	141.31(14)
Ga(1)−O(21)−P(2)	123.41(11)	Ga(2)−O(34)−P(3)	131.62(15)
Ga(1)−O(32)−P(3)	133.26(12)	Ga(3)−O(14)−P(1)	133.12(12)
Ga(2)−O(11)−P(1)	128.55(12)	Ga(3)−O(22)−P(2)	123.98(11)
Ga(2)−O(12)−P(1)	134.68(13)	Ga(3)−O(33)−P(3)	130.08(11)

Monobidentate Oxalate				Bisbidentate Oxalate	
C(1)−O(1)	1.288(3)	C(1)−O(3)	1.231(3)	C(3)−O(5) 2×	1.261(3)
C(2)−O(2)	1.279(3)	C(2)−O(4)	1.239(3)	C(3)−O(6) 2×	1.251(3)

of a single crystal selected from the sample after heating at 250 °C confirmed the loss of all water molecules and the stability of the framework. The loss of water results in a small change in the unit cell parameters with a decrease of 16.3 Å^3 in volume: a = 9.002(2) Å, b = 9.173(2) Å, c = 13.291(4) Å, α = 75.39(2)°, β = 77.75(2)°, γ = 78.59(2)°, and V = 1025.6(4) Å^3 (at 228 K). This dehydration is reversible as the dehydrated phase partially reabsorbs water. TGA analysis of a sample of the completely dehydrated phase after exposure to a 100% relative humidity atmosphere shows that the compound has regained 1.25 H_2O. This dehydration−hydration process can be repeated many times. X-ray analysis of a single crystal after rehydration led to a unit cell: a = 9.04(1) Å, b = 9.15(2) Å, c = 13.37(3) Å, α = 74.80(6)°, β = 78.61(5)°, γ = 78.3(1)°, V = 1032(3) Å^3 (at 228 K). The second mass loss (24.8%) occurs between 275 and 800 °C and corresponds to the loss of hydroxyls, oxalates, and the amine, leading to the formation of $GaPO_4$ (calcd 32.5%). TGA data are submitted as Supporting Information.

NMR Spectrosocpy. *^{71}Ga NMR.* At high field the gallium spectrum shows three components, at −21.7, −19.8, and 111.3 ppm at an approximate ratio of 1:1:1 (Figure 5). This is in agreement with the two octahedrally coordinated Ga(1) and Ga(3), for the sites at −21.7 and −19.8 ppm. The peak at 111 ppm is assigned to the tetrahedrally coordinated Ga(2).

^{31}P NMR. The phosphorus spectrum exhibits three components with respective chemical shifts at −0.2, −4.15, and −7.7 ppm in a 1:1:1 ratio (Figure 6), consistent with the structural model determined from the XRD structural analysis. The empirical relation between chemical shifts and mean ⟨POM⟩ angle leads to a tentative assignment at −0.2 ppm for P(2) with ⟨POM⟩ = 124.9°, −4.15 ppm for P(3) with ⟨POM⟩ =

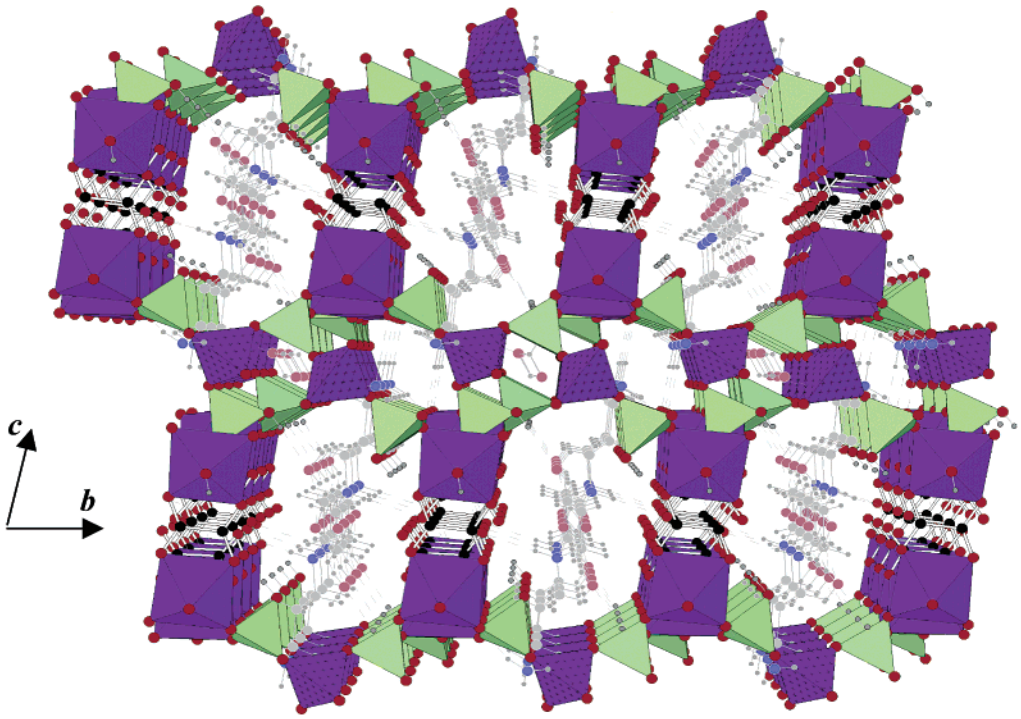

Figure 2. A polyhedral perspective view of the 3D framework of **1** along the [100] direction showing the double layers bridged by oxalate ligands. GaO_6, purple; GaO_4, purple dashed; HPO_4, green; carbon, black; oxygen, red; nitrogen, blue.

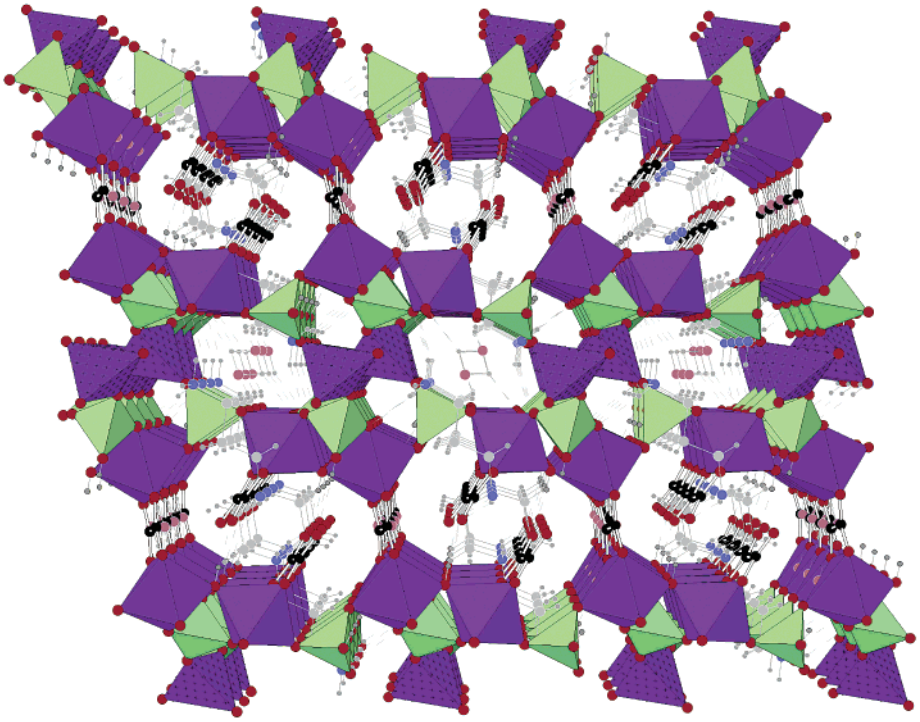

Figure 3. A polyhedral perspective view of the 3D framework of **1** along the [010] direction showing the mono-bidentate oxalate and the stacking of the amine cation and water molecules in the channels. GaO_6, purple; GaO_4, purple dashed; HPO_4, green; carbon, black; oxygen, red; nitrogen, blue.

128.7°, and −7.7 ppm for P(1) with ⟨POM⟩ = 132.3°. The central component assigned to P(3) is broader and can be decomposed into two lines of half the multiplicity at −3.7 and −4.6 ppm. The lowering of symmetry on P(3) may be local or nonlocal.

^{13}C NMR. The CPMAS NMR experiment leads to well-resolved carbon spectra for the oxalate sites (Figure 7) with three nonequivalent carbon sites at 168.3, 167.4, and 165.6 ppm. They are in a 1:1:1 ratio, confirming the multiplicity observed by diffraction analysis. The two peaks at 168.3 and 167.4 ppm are close to each other and can be assigned to C(1) and C(2), and the peaks at 165.6 ppm can be assigned to C(3). The latter peak can be decomposed into two lines of 0.5:0.5 ratio as for P(3) in phosphorus NMR. This should be considered as a local or global lowering of symmetry that will be

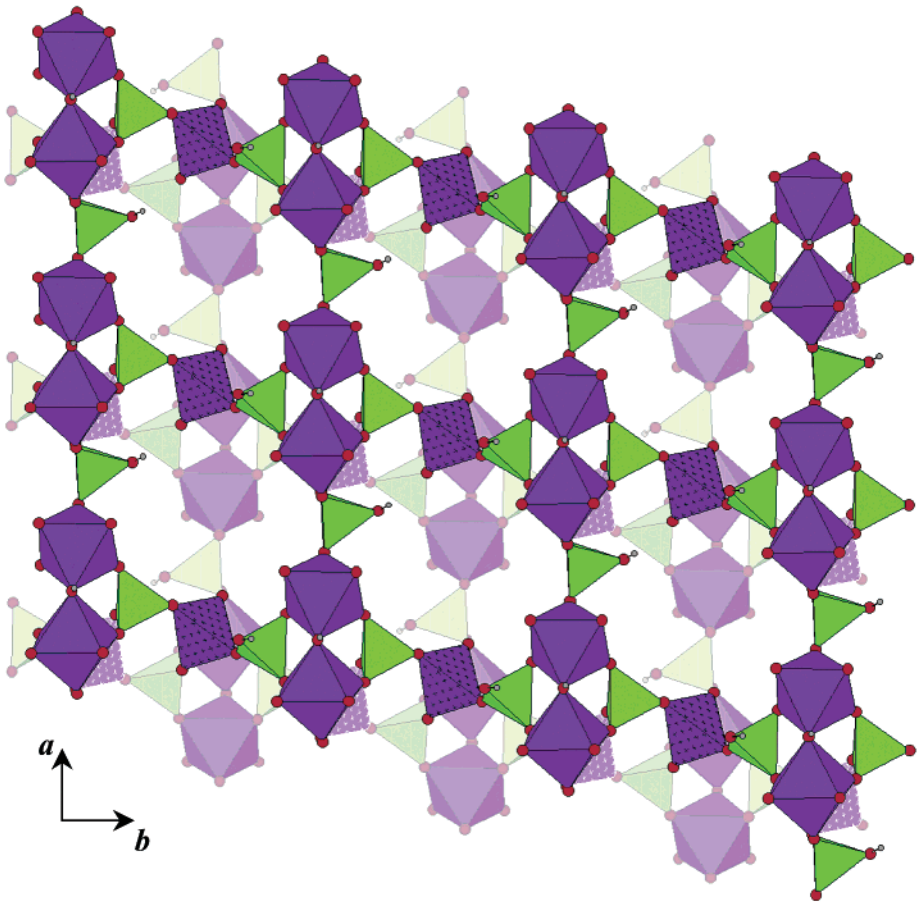

Figure 4. A projection on the (*ab*) plane of a fragment of one double layer showing the chains (running along the *a*-axis) connected to each other through GaO_4 tetrahedra (purple dashed). The two single layers are distinguished in color.

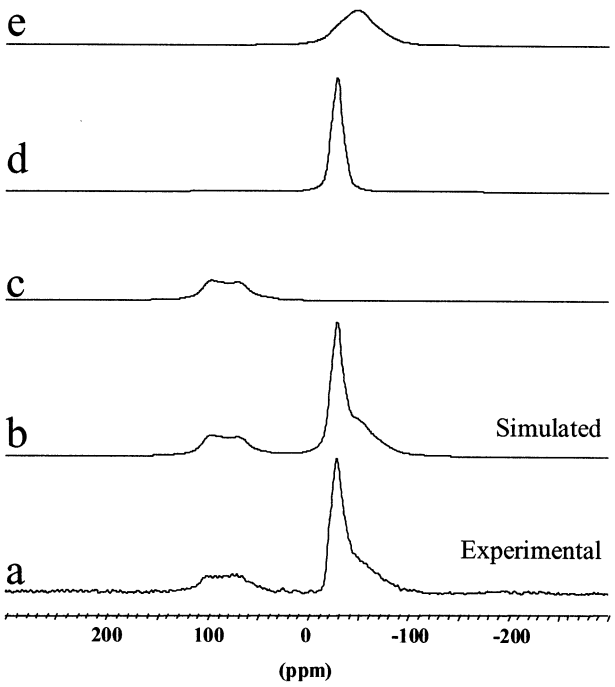

Figure 5. ^{71}Ga MAS spectrum: (a) Experimental MAS. (b) Simulated assuming three components as (c), (d), and (e) with a 0.25:0.385:0.365 ratio. (c) $\delta_{iso} = 111$ ppm, $C_Q = 8.98$ MHz, $\eta_Q = 0$. (d) $\delta_{iso} = -19.8$ ppm, $C_Q = 4.52$ MHz, $\eta_Q = 0.7$. (e) $\delta_{iso} = -21.7$ ppm, $C_Q = 7.94$ MHz, $\eta_Q = 0.7$.

discussed later. The remaining carbon lines correspond to the equivalent signals in solution with a splitting of multiplicity for the carbon of the ring (C(14) and C(15)).

Table 3. Hydrogen-Bonding Interactions in $[N_4C_{10}H_{28}][Ga_6(OH)_2(PO_4)_2(HPO_4)_4(C_2O_4)_3]\cdot 3.5H_2O$

donor atom (D)	acceptor atom (A)	D···A (Å)	H···A (Å)	D−H···A angle (deg)
N(1)−H(1N1)	O(24)	2.956(4)	2.50	111
N(1)−H(1N1)	O(12)	3.356(4)	2.56	146
N(1)−H(2N1)	O(21)	2.871(3)	1.99	157
N(1)−H(3N1)	O(22)	3.043(4)	2.12	161
N(1)−H(3N1)	O(34)	2.995(4)	2.42	118
N(2)−H(1N2)	O(4)	3.019(3)	2.23	152
N(2)−H(1N2)	O(2)	3.121(3)	2.46	134
O(7)−H(7)	O(4)	2.726(3)	1.99	168
O(23)−H(23)	O(7)	2.971(3)	2.43	126
O(23)−H(23)	O(3)	3.181(3)	2.45	152
O(31)−H(31)	O(1w)	2.807(5)	2.06	176
O(1w)−H(1w1)	O(3w)	2.58(1)	1.89	131
O(1w)−H(1w1)	O(23)	3.100(1)	2.59	117
O(1w)−H(1w2)	O(23)	3.100(5)	2.62	118
O(2w)−H(2w)	O(13)	2.867(6)	2.17	128
O(3w)−H(3w)	O(1w)	2.304(5)	1.65	134

$^1H/^2H$ NMR. The hydrogen spectrum (^{1}H) (Figure 8) exhibits three components that are assigned to CH_2, NH_3, NH, and H_2O. The spectra cannot resolve the different types of CH_2. The NH_3 signals resonate at 7.9 ppm, as usually observed in protonated amines in solution as well as in ammonium templates in microporous solids. H_2O signals resonate around 4.5 ppm. Spectra obtained for deuterated samples show only two signals at 7.9 and 4.6 ppm. Assignment of NH signals to 7.9 would lead to a very large excess of water at 4.6 ppm. Assigning NH at about 5 ppm leads to a consistent

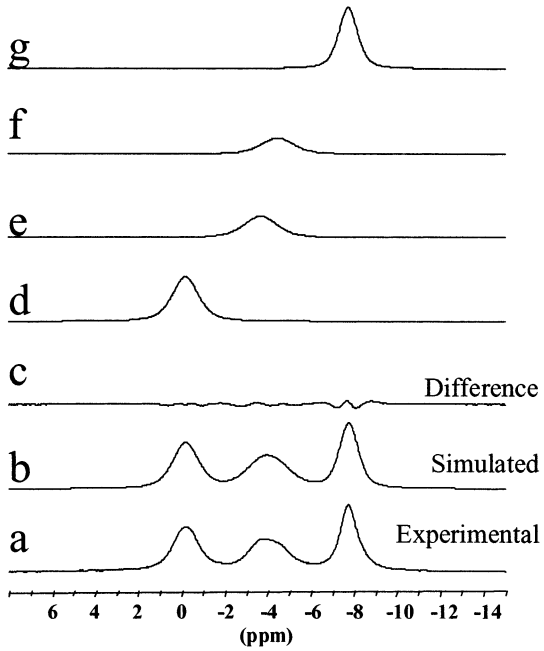

Figure 6. ^{31}P spectrum: (a) Experimental MAS. (b) Simulated assuming four components as (d), (e), (f), and (g) with a 1:0.5:0.5:1 ratio. (c) Difference between (a) and (b). (d) $\delta_{iso} = -0.2$ ppm. (e) $\delta_{iso} = = -3.7$ ppm; (f) $\delta_{iso} = = -4.5$ ppm. (g) $\delta_{iso} = -7.7$ ppm.

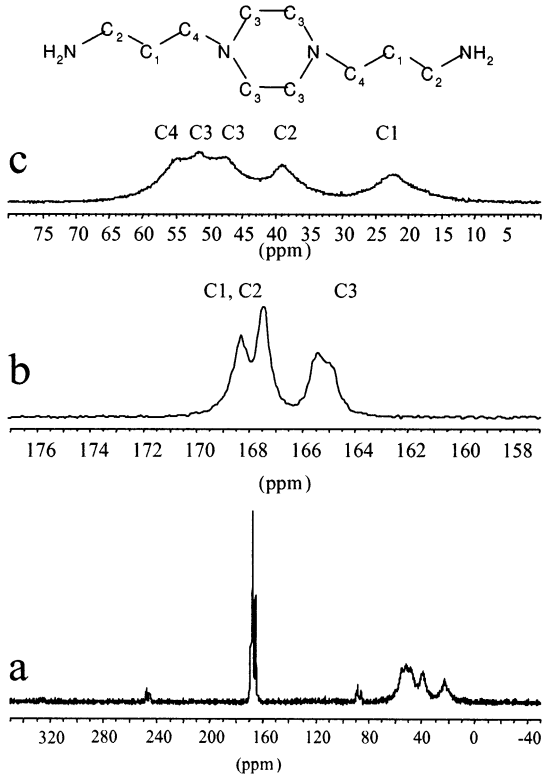

Figure 7. ^{13}C CPMAS spectrum: (a) Full spectral width. (b) Expansion around the oxalates sites, carbon numbering is the crystal scheme numbering used in structure description. (c) Expansion in the region of the 1,4-bis(3-aminopropyl)piperazine. The carbon numbering in (c) is the numbering scheme of the molecule drawn on top of the figure.

ratio between NH_3 and NH of 6:2. ^{2}H NMR spectra in static conditions (Figure 9) confirm these results. Two intense signals are obtained, with quadrupolar interac-

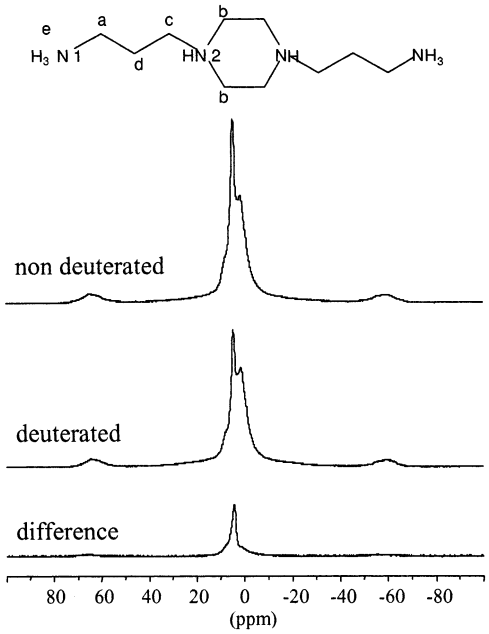

Figure 8. ^{1}H spectrum: The 1,4-bis(3-aminopropyl)piperazine ^{1}H labeling has been plotted on top of the figure. H_{3N1} and H_{N2} as well as H_2O are exchangeable during deuteuration. The spectrum is decomposed with three components at 7.9 ppm, 4.6 ppm, and about 1.6 ppm. NH_3 resonates at 7.9 while NH and water hydrogen atoms resonate at 4.6 ppm and the other CH_2 are not resolved at 1.6 ppm.

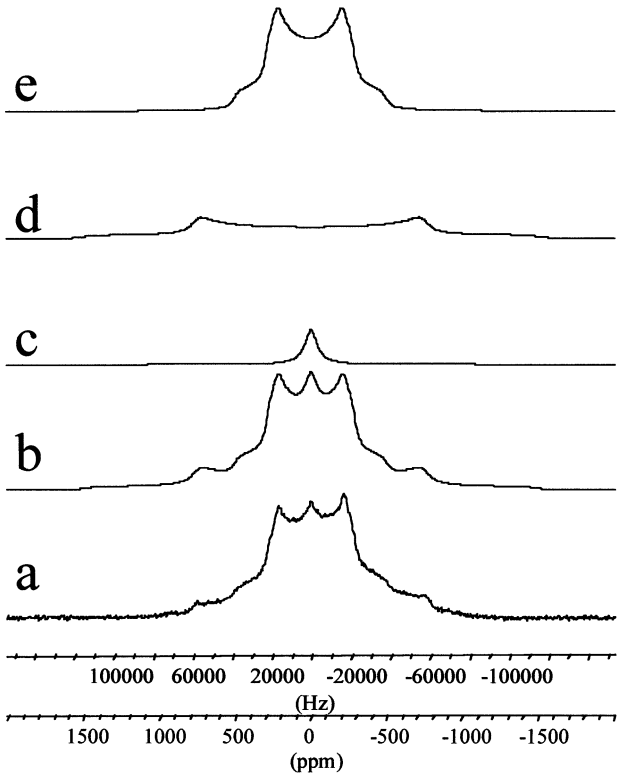

Figure 9. ^{2}H spectrum: (a) is the static deuterium spectrum. (b) Its simulation assuming three components, two major (d) and (e) and some residual adsorbed water in (c). Both ppm and Hz scale are plotted for convenience. CH_2's are not exchanged; only NH_3, NH, and H_2O could exhibit deuteron signals.

tions of about 51 and 153 Hz, most probably due to NH_3 and H_2O. NH is certainly too weak to be detected, for it

is of the lowest quantity with the largest expected quadrupolar interaction (more than 200 kHz).

Overall, the agreement between the structural model obtained from XRD analysis and the nonequivalent sites observed by NMR is good. However, for two clear cases, P(3) in phosphorus NMR and C(3) in carbon NMR, a lower symmetry is observed. Detailed inspection of the environment of these two sites shows that P(3) has a water molecule O(2w) nearby which partially occupies two alternative sites and C(3) has a water molecule O(3w) nearby which occupies two closely spaced sites with C(3)−O(3w) = 3.5 and 4.2. As shown in a forthcoming study,[56] such a situation leads to a local "small water pool" that influences the chemical shift of the surrounding atoms. The possible situation is midway between a discrete localized situation with well-defined nonequivalent sites and a continuous distribution of sites. Here, we are most probably in the case where the water pool made of two water molecules (definitely a very small pool!) leads to a local splitting of P(3) and C(3) into two sites. However, the influence of these small modulations of the structure does not affect the overall periodicity of the crystal that remains well-described by the centrosymmetric $P\bar{1}$ space group.

Conclusion and Comparison with Known Structures

Compound **1** is characterized by the presence of two types of oxalates, one acts as a mono-bidentate and the second acts as a bis-bidentate ligand. To the best of our knowledge, this is the first example where such a combination is observed. However, its structure has features common to other metal phosphatooxalates built of metal phosphate layers pillared by oxalate anions to form a 3D framework with channels where a structure-directing amine is located. Examples include $[C_4H_{12}N_2][In_2(HPO_4)_3(C_2O_4)]\cdot H_2O$,[51] $[N_2C_4H_{12}]_{0.5}[Fe_2(HPO_4)(C_2O_4)_{1.5}]$,[39] $[NH_3(CH_2)_2NH_3]_{1.5}[Fe_3(PO_4)(HPO_4)_3(C_2O_4)_{1.5}]\cdot xH_2O$,[40] and $[C_5H_{14}N_2][Fe_2(HPO_4)_3(C_2O_4)]$.[36]

The mono-bidentate coordination mode has been observed in the 1D $[NH_3(CH_2)_2NH_3]_{2.5}[Al_4H(HPO_4)_4(H_2PO_4)_2(C_2O_4)_4]$[46] and $[C_4H_{12}N_2][VO(HPO_4)(C_2O_4)]$.[29] The bis-bidentate coordination mode in which the oxalate ligand bridges two metal centers either within the metal phosphate layers as is the case in the two original gallium phosphatooxalates previously reported by Lii et al.[48,49] or between layers is predominately observed in these hybrid materials. The presence of the mono-bidentate oxalate ligand with two C−O functional groups that are pendant within compound (**1**) is an additional step toward the goal of the preparation of open-framework materials with accessible functional groups[57] and has prompted our current work on studying the effects of bidentate ligands with other functionalities on the structural and chemical properties of this class of materials.

Acknowledgment. This material is based upon work supported by the National Science Foundation under Grant DMR-0070915. Acknowledgment is made to the donors of the Petroleum Research Fund, administered by the American Chemical Society ACS-PRF#36080-AC5, for partial support of this work.

Supporting Information Available: One X-ray crystallographic file (CIF) and tables of NMR acquisition parameters and two figures showing the TGA under air and under N_2 (PDF). This material is available free of charge via the Internet at http://pubs.acs.org.

CM020389K

(56) Beitone, L.; Marrot, J.; Loiseau, T.; Férey, G.; Henry, M.; Taulelle, F., in preparation.

(57) Zhu, J.; Bu, X.-H.; Feng, P.-Y.; Stucky, G. D. *J. Am. Chem. Soc.* **2000**, *122* (46), 11563.